Available online at www.sciencedirect.com
SCIENCE DIRECT®
International Journal of Heat and Mass Transfer 48 (2005) 373–383
International Journal of HEAT and MASS TRANSFER
www.elsevier.com/locate/ijhmt

# Study on the efficiency of effective thermal conductivities on melting characteristics of latent heat storage capsules

Yasuaki Shiina [a,*], Terumi Inagaki [b,1]

[a] Department of Advanced Nuclear Heat Technology, Japan Atomic Energy Research Institute, 3607 Oarai-machi, Higashi-Ibaraki-gun, Ibaraki-ken 311-1394, Japan
[b] Department of Mechanical Engineering, Ibaraki University, Naka-Naruasawa-cho, Hitachi-shi, Ibaraki-ken 316-8511, Japan

Received 1 April 2003; received in revised form 9 July 2004

**Abstract**

Improvement of the thermal conductivity of a phase change materials (PCM) is one effective technique to reduce phase change time in latent heat storage technology. Thermal conductivity is improved by saturating porous metals with phase change materials. The influence of effective thermal conductivity on melting time is studied by analyzing melting characteristics of a heat storage circular capsule in which porous metal saturated with PCM is inserted. Numerical and approximate analyses were made under conditions where there are uniform or non-uniform heat transfer coefficients around the cylindrical surface. Four PCMs ($H_2O$, octadecane, $Li_2CO_3$, NaCl) and three metals (copper, aluminum and carbon steel) were selected as specific materials. Porosities of the metals were restricted to be larger than 0.9 in order to keep high capacity of latent heat storage. Results show that considerable reduction in melting time was obtained, especially for low conductivity PCMs and for high heat transfer coefficient. Melting time obtained by approximate analysis agrees well with numerical analysis. A trial estimation of optimum porosity is made balancing the desirable conditions of high latent heat capacity and reduction of melting time. Optimum porosity decreases with increase in heat transfer coefficient.


*Keywords:* Heat storage; Melting; Phase change; Heat transfer; Thermal conductivity; Circular cylinder; PCM

## 1. Introduction

In recent years, latent heat storage technology has been widely studied to develop compact heat storage systems with high energy density and small temperature difference. For the application of the latent heat storage technique, improvement of heat transfer during phase change is required because heat transfer in present latent heat storage systems is comparatively low. In particular, heat transfer deteriorates during solidification because heat is transferred only by thermal conduction and thermal conductivity of phase change material (PCM) is very small. If phase change time is reduced, heat generated by electric power plants in the night can be stored and used for generation of electricity in the daytime.

Several techniques have been applied to improve heat transfer during solidification. First, use of a finned

* Corresponding author. Tel.: +81 29 264 8705; fax: +81 29 264 8710.
*E-mail addresses:* shiina@spa.oarai.jaeri.go.jp (Y. Shiina), inagaki@mech.ibaraki.ac.jp (T. Inagaki).
[1] Tel./fax: 81 294 38 5044.

0017-9310/$ - see front matter © 2004 Elsevier Ltd. All rights reserved.
doi:10.1016/j.ijheatmasstransfer.2004.07.043

**Nomenclature**

| | |
|---|---|
| $Bi_{fl}$, | Biot number = $D_o h_0/(\lambda_{fl})_{ef}$ |
| $Bi_{ml}$, $Bi_{ms}$ | modified Biot number $Bi_{ml} = D_o h/(\lambda_{fl})_{ef}$, $Bi_{ms} = D_o h/(\lambda_{fs})_{ef}$ |
| $Bi_w$ | $Bi_w = D_o h_0/\lambda_w$ |
| $c$ | specific heat |
| $D_i$, $D_o$ | inner and outer diameter of a circular capsule |
| $G$ | solid fraction |
| $h_0$, $h(\theta)$ | uniform and non-uniform heat transfer coefficient on the surface of a circular capsule, respectively |
| $h$ | effective heat transfer coefficient (Eq. (2)) |
| HTF | heat transfer fluid |
| $L$ | latent heat |
| $Nu$ | Nusselt number = $D_o h_0/\lambda_g$ |
| $R_i$, $R_o$ | inner and outer radius of a circular capsule, respectively |
| $Pr$ | Prandtl number |
| $q$ | surface heat flux |
| $Re$ | Reynolds number = $UD_o/v$ |
| $s$ | radius of solid phase |
| $St$ | Stephan number = $c(T_\infty - T_f)/L$ |
| $t_e$ | melting time of solid PCM from $T = T_f$ |
| $t_f$ | time for temperature rise of solid PCM from $T_i$ to $T_f$ |
| $t_t$ | total melting time |
| $T_f$, $T_i$ | melting temperature and initial temperature, respectively |
| $T_w$, $T_1$, $T_\infty$ | outer surface temperature of a capsule, inner surface temperature of a capsule, and temperature of heat transfer fluid, respectively |
| $U$ | velocity of heat transfer fluid |
| $\theta$ | angle measured from stagnation point |
| $\theta_f$ | non-dimensional temperature $\theta_f = (T_f - T_\infty)/(T_i - T_\infty)$ |
| $\varepsilon$ | porosity |
| $\rho$ | density |
| $\kappa$ | thermal diffusivity |
| $v$ | kinematic viscosity |
| $\lambda$ | thermal conductivity |
| $\tau$ | non-dimensional time |

*Subscripts*

| | |
|---|---|
| f | phase change material, f = fl or f = fs |
| fl, fs | liquid and solid phase of PCM |
| g | heat transfer fluid |
| ef | effective value |
| m | metal |

surface in a PCM [1,2], second, use of PCM enclosed in capsules to reduce heat transfer resistance [3,4], third, improvement of effective thermal conductivity by the use of high thermal conductivity porous materials saturated with PCM [5–7]. There are experiments and analyses dealing with the first and second techniques [1,4]. Also, effectiveness of these techniques is discussed in these studies. For the third technique, measurement of thermal conductivity of PCM contained in porous metals and limits in the onset of natural convection have been studied [6,7]. However, there has hardly been any consideration and comparison of techniques with regard to reduction in phase change time.

In the present study, the influence of effective thermal conductivity on melting characteristics for PCM enclosed in circular cylindrical capsules is studied mainly by numerical techniques, and availability of the technique are discussed by the comparison with the results of finned surface. In the past, heat transfer characteristics of heat storage capsules have been estimated assuming constant heat transfer rate on the capsule surface [3]. In practice, however, heat transfer rate on the surface is non-uniform, and non-uniformity might exert large effects on the phase change characteristics. Difference in melting characteristics between uniform and non-uniform heat transfer rate are also considered in the present study.

## 2. Analysis

Quasi-steady treatment is possible [8] in the case of large latent heat relative to sensible heat, i.e., for small Stephan number. Analytical solutions are very effective in comprehending the influence of effective thermal conductivity on melting characteristics systematically. Then, approximate and numerical analyses are performed to consider the accuracy and application limits of the approximate analysis and to clarify the effect of non-uniform heat transfer coefficient on melting.

The physical system is shown in Fig. 1. Melting characteristics of PCM enclosed in a circular cylindrical capsule put in a forced convection current of heat transfer fluid (HTF) with the velocity $U$ was analyzed. The outer and inner diameter of the circular capsule are $D_o$ and $D_i$, respectively. Initial temperature of the PCM and bulk temperature of the HTF are $T_i$ ($<T_f$) and $T_\infty$, respectively. Porous metal saturated with PCM (hereafter called composite PCM) is set in the circular capsule.

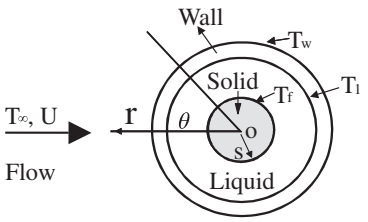


Fig. 1. Physical system of the present analysis.

In the analysis, natural convection of liquid PCM was neglected.

### 2.1. Approximate analysis

Analysis was performed based on the following assumptions:

(a) Stephan number $St$ is small;
(b) heat which is input to the capsule is used only for phase change

Assumption (b) will be approximately correct for initial temperature to be equal to $T_f$. Analysis was performed by dividing the melting process into two stages: (1) sensible heat generation during temperature change from initial temperature to melting temperature; (2) latent heat melting process of composite PCM.

#### 2.1.1. Sensible heat generation during temperature change from initial to melting temperature

Modified Biot number is defined using the uniform heat transfer coefficient $h_0$ on the capsule surface:

$$Bi_{ml} = \frac{D_o h}{(\lambda_{fl})_{ef}} = \frac{Bi_{fl}}{1 + (1/2)Bi_w \ln(D_o/D_i)}$$
$$Bi_{ms} = Bi_{ml}\frac{(\lambda_{fl})_{ef}}{(\lambda_{fs})_{ef}} \quad (1)$$

where

$$h = \{(1/h_0) + (D_o/2\lambda_w)\ln(D_o/D_i)\}^{-1} \quad (2)$$

$$Bi_{fl} = D_o h_0/(\lambda_{fl})_{ef}, \quad Bi_w = D_o h_0/\lambda_w \quad (3)$$

When heat transfer resistance of the capsule wall is very small, the outer surface temperature of the capsule can be obtained as follows [9]:

$$\frac{T_w - T_\infty}{T_i - T_\infty} = \sum_{n=1}^{\infty} \frac{2\beta R_i}{\alpha_n^2 + (\beta R_i)^2} e^{-\alpha_n^2 \frac{(\kappa_{fs})_{ef}\cdot t}{R_i^2}} \quad (4)$$

In Eq. (4), $\beta = h/(\lambda_{fs})_{ef}$ where $\beta R_i = Bi_{ms}R_i/2R_o$. $\alpha_n$ is the root of $\beta R_i = xJ_1(x)/J_0(x)$. When $\beta$ is small (i.e., $Bi_{ms}$ is small), the right-hand side of Eq. (4) is determined by $\alpha_1$ because $\alpha_1 \ll \alpha_n$ ($n = 2, 3, \ldots$). In this case, $\alpha_1$ can be calculated using $\alpha_1 = 2\sqrt{2\beta R_i/(\beta R_i + 4)}$. In the case where $Bi_{ms}$ is smaller than unity, the time at which the temperature of capsule surface becomes equal to $T_f$ can be regarded as the time at which temperature of the whole capsule becomes equal to $T_f$. In this case, $t_f$ can be expressed using $\theta_f = (T_f - T_\infty)/(T_i - T_\infty)$ as

$$\tau_f = \frac{(\kappa_{fl})_{ef}\cdot t_f}{D_i^2} = -\frac{1}{16}\frac{(\kappa_{fl})_{ef}}{(\kappa_{fs})_{ef}}\left\{1 + \frac{(\lambda_{fs})_{ef}}{(\lambda_{fl})_{ef}}\frac{D_o}{D_i}\frac{4}{Bi_{ml}}\right\}\ln\theta_f \quad (5)$$

#### 2.1.2. Latent heat melting process

Liquid temperature, outer surface temperature and temperature difference between outer and inner surfaces for the case of the liquid solid boundary $r = s$ can be expressed as follows:

$$\frac{T - T_f}{T_\infty - T_f} = \frac{\ln(r/s)}{2/Bi_{ml} + \ln(R_i/s)} \quad \text{(Liquid)} \quad (6)$$

$$\frac{T_\infty - T_w}{T_\infty - T_f} = \frac{2/Bi_{fl}}{2/Bi_{ml} + \ln(R_i/s)} \quad \text{(Outer surface)} \quad (7)$$

$$\frac{T_w - T_l}{T_\infty - T_f} = \frac{\{(\lambda_{fl})_{ef}/\lambda_w\}\ln(D_o/D_i)}{2/Bi_{ml} + \ln(R_i/s)} \times (\text{Temperature difference between inner and outer surfaces}) \quad (8)$$

On the basis of assumption (b), the relation between $t$ and liquid solid boundary $r = s$ can be obtained as follows:

$$\frac{(\kappa_{fl})_{ef}\cdot t}{D_i^2} = \frac{1}{16St}\left(1 + \frac{4}{Bi_{ml}}\right)\left[\left\{1 - \left(\frac{s}{R_i}\right)^2\right\} + \frac{2}{1 + 4/Bi_{ml}}\left(\frac{s}{R_i}\right)^2 \ln\frac{s}{R_i}\right] \quad (9)$$

When melting is finished, melt time $t_e$ is written as follows:

$$\tau_e = \frac{(\kappa_{fl})_{ef}t_e}{D_i^2} = \frac{1}{16St}\left(1 + \frac{4}{Bi_{fl}} + \frac{2(\lambda_{fl})_{ef}}{\lambda_w}\ln\frac{D_o}{D_i}\right) \quad (10)$$

Therefore, the non-dimensional form of total melting time $\tau_t$ can be obtained by summing $\tau_e$ and $\tau_f$:

$$\tau_t = \tau_e + \tau_f = \frac{1}{16St}\left(1 + \frac{4}{Bi_{fl}} + \frac{2(\lambda_{fl})_{ef}}{\lambda_w}\ln\frac{D_o}{D_i}\right) - \frac{1}{16}\frac{(\kappa_{fl})_{ef}}{(\kappa_{fs})_{ef}}\left\{1 + \frac{(\lambda_{fs})_{ef}}{(\lambda_{fl})_{ef}}\frac{D_o}{D_i}\frac{4}{Bi_{ml}}\right\}\ln\theta_f \quad (11)$$

### 2.2. Numerical analysis

The heat conduction equation written as follows is integrated with the boundary conditions involving the surface heat transfer coefficient:

$$\rho c\frac{\partial \overline{T}}{\partial t}=\lambda\left(\frac{\partial^2\overline{T}}{\partial r^2}+\frac{1}{r}\frac{\partial \overline{T}}{\partial r}+\frac{1}{r^2}\frac{\partial^2\overline{T}}{\partial\theta^2}\right)+\rho L\frac{\partial G}{\partial t} \tag{12}$$

where $\overline{T}=T-T_{\mathrm{f}}$ and $G$ means solid fraction of PCM, therefore $G=0$ and 1 correspond to complete liquid and complete solid states, respectively. For the cases of no phase change and uniform heat transfer coefficient on the surface, both $\partial G/\partial t$ and $\partial/\partial\theta$ can be set as zero.

Initial and boundary conditions are as follows:

$$\begin{aligned} &t\leqslant 0; \quad T=T_{\mathrm{i}}\\ &t>0,\ r=R_{\mathrm{o}}; \quad q=h(\theta)\cdot(T_{\mathrm{w}}-T_{\infty})\\ &\qquad\qquad\ \text{or } q=h_0(T_{\mathrm{w}}-T_{\infty}) \end{aligned} \tag{13}$$

where $h(\theta)$ is the non-uniform heat transfer coefficient on a surface of a circular cylindrical capsule. The heat transfer coefficient $h(\theta)$ is dependent on the flow pattern around the cylindrical capsule. The flow pattern around a cylinder in a bank of cylinders is determined by the arrangement and geometrical parameters of the bank. There are two specific arrangements of the bank, i.e. arrangement in straight lines and a staggered arrangement. In the case of straight line arrangement, heat transfer coefficient at a stagnation point behind the first row is reduced because it is situated in the wake of the upstream cylinders. On the other hand, in case of the staggered arrangement, the heat transfer coefficient on all capsule surfaces is roughly similar to the first row [10]. The ratio of maximum and minimum heat transfer coefficient is 3–4 on the surfaces of circular cylinders in a bank [10], whereas it is 5–6 for a single circular cylinder in a uniform flow [11]. Angular distribution of heat transfer coefficient around a circular cylindrical capsule in an arbitrary arrangement was represented by that of a circular cylinder in a uniform flow because under the condition the effect of non-uniformity of heat transfer coefficient is the maximum on the melting process. Heat transfer coefficients were obtained from the experiment of Eckert [11] for low Reynolds numbers and the correlation of Schmidt and Wenner [12] for high Reynolds numbers. The experimental results of Eckert are expressed by the following approximations:

$$\begin{aligned} &Nu=1.02Re^{0.5}Pr^{0.4}\{1-(\theta/130)^2\}\\ &\quad 0^\circ\leqslant\theta\leqslant 120^\circ, 20\leqslant Re\leqslant 1000\\ &Nu=0.366Re^{0.5}Pr^{0.4}\{(\theta/90)-1\}^{0.6}\\ &\quad (120^\circ\leqslant\theta\leqslant 180^\circ) \end{aligned} \tag{14}$$

The correlation of Schmidt and Wenner are expressed as follows:

$$\begin{aligned} &Nu=1.14Re^{0.5}Pr^{0.4}\{1-(\theta/90)^3\}\\ &\quad 0^\circ\leqslant\theta\leqslant 86.5^\circ, 10^3\leqslant Re\leqslant 10^5\\ &Nu=0.196Re^{2/3}Pr^{0.4}\{(\theta-77)/103\}^{2/3}\\ &\quad (86.5^\circ\leqslant\theta\leqslant 180^\circ) \end{aligned} \tag{15}$$

The ratios of Nusselt number at the front and the back of a circular cylinder obtained by Eqs. (14) and (15) are 2.5 and 1.1 respectively. Therefore, non-uniformity is high for low Reynolds numbers.

For the analysis based on a uniform heat transfer coefficient, the above equations were averaged around the surface, which yielded the following average Nusselt number:

$$\begin{aligned} &Nu=0.591Re^{0.5}Pr^{0.4}\quad 20\leqslant Re\leqslant 1000\\ &Nu=(0.425Re^{0.5}+0.065Re^{2/3})Pr^{0.4}\quad 10^3\leqslant Re\leqslant 10^5 \end{aligned} \tag{16}$$

The procedure of the calculation is as follows:

(1) Temperature was calculated without consideration of phase change.
(2) When calculated temperature $T$ of a control volume with $G>0$ exceeds $T_{\mathrm{f}}$, excess heat $Q$ corresponding to $T-T_{\mathrm{f}}$ is calculated.
(3) If $Q$ is smaller than total latent heat of the control volume, temperature of the control volume is maintained at $T_{\mathrm{f}}$, and $G$ is corrected corresponding to $Q$.
(4) If $Q$ is larger than the latent heat, $G$ is zero and the temperature of the control volume is corrected.

In the preliminary calculation, the number of mesh was changed from 20 to 100 in the $r$-direction for the case of uniform heat transfer and the difference in results was within 0.5%. In the end, 50 mesh in the liquid and 10 mesh in the wall were adopted for the uniform heat transfer coefficient, and $20\times 32$ mesh in the $r-\theta$ directions in the liquid and 2 mesh in the $r$-direction in the wall were adopted for the non-uniform heat transfer coefficient.

### 2.3. Analytical condition

Analysis was performed for commercially used PCM and metal foam of commercially used metal. Water, octadecane, $Li_2CO_3$ and NaCl were selected as PCMs and copper, aluminum and carbon steel as metal foam matrices. Thermal properties of the above materials are shown in Tables 1 and 2. Metal foam matrices can be regarded as a cubic lattice of rectangular wire whose cross section is square. Metal foam of carbon steel is not manufactured as yet, but cubic lattice of carbon steel was selected because carbon steel is usable over a wide range of temperatures, and production of a cubic lattice seems to be not difficult. Thermal properties of the composite PCM were obtained by following equations:

$$\begin{aligned} &\text{(a) Density}: \quad (\rho)_{\mathrm{ef}}=\rho_{\mathrm{f}}\varepsilon+\rho_{\mathrm{m}}(1-\varepsilon)\\ &\text{(b) Specific heat}: \quad (c)_{\mathrm{ef}}=\{\rho_{\mathrm{f}}\varepsilon c_{\mathrm{f}}+\rho_{\mathrm{m}}(1-\varepsilon)c_{\mathrm{m}}\}/(\rho)_{\mathrm{ef}}\\ &\text{(c) Latent heat}: \quad (L)_{\mathrm{ef}}=\rho_{\mathrm{f}}L\varepsilon/(\rho)_{\mathrm{ef}} \end{aligned} \tag{17}$$

Table 1
Thermal properties of the phase change materials used in the analysis (l: liquid, s: solid)

| | $T_f$ (°C) | $\lambda_{fl}$ (W/m K) | $\rho$ (kg/m$^3$) | $C_P$ (kJ/kg K) | L (kJ/kg) |
|---|---|---|---|---|---|
| $H_2O$ | | 0.595 (l) | 1000 | 4.19 (l) | |
| | 0 | 2.2 (s) | | 2.0 (s) | 333 |
| Octadecane | 28 | 0.15 (l) | 850 | 2.2 (l) | |
| | | 0.42 (s) | | 1.8 (s) | 243 |
| $Li_2CO_3$ | 723 | 1.97 (l) | 1840 | 2.51 (l) | |
| | | | | | 556 |
| NaCl | 800 | 1.26 (l) | 1560 | 1.23 (l) | |
| | | | | | 483 |

Table 2
Thermal properties of metals

| | $\rho$ (kg/m$^3$) | $c$ (kJ/kg K) | $\lambda_m$ (W/m K) |
|---|---|---|---|
| Copper | 8880 | 0.386 | 398 |
| Aluminum | 2690 | 0.905 | 237 |
| Carbon steel | 7850 | 0.465 | 43 |

(d) Thermal conductivity: when a cubic lattice has unit length and the side width of the square wire is $x$, porosity and effective thermal conductivity can be obtained as follows under the assumption of one-dimensional heat flow [13]:

$$1-\varepsilon = 3x^2 - 2x^3$$

$$(\lambda_f)_{ef} = \lambda_m x^2 + \lambda_f (1-x)^2 + 2(1-x)x\left\{\frac{\lambda_m \lambda_f}{\lambda_m(1-x)+\lambda_f x}\right\} \quad (18)$$

From the view point of high heat storage capacity, porosity is desired to be near unity. Therefore, in the present study, analysis was performed for $\varepsilon = 0.9$, 0.95, 0.98, 1.0. Relation between thermal conductivities of pure and composite PCMs are shown in Fig. 2. Effective thermal conductivities of composite PCM of copper foam matrices saturated with octadecane and $Li_2CO_3$ with $\varepsilon = 0.9$ show thermal conductivities 100 and 8.5 times as high as that of the pure PCM, respectively.

Acrylic resin and copper were used as the capsule wall for their thermal properties. Outer and inner diameters of the capsule were set as 6.6 mm and 6 mm, i.e., wall thickness was 0.3 mm. The Reynolds number of the HTF was variously set at 300, 3000 and 7500. The case of $Re = 300$ is that of high non-uniformity of heat transfer coefficient on the capsule surface, and the cases of $Re = 3000$ and 7500 are those of small non-uniformity. Air, helium and water were selected as the HTF

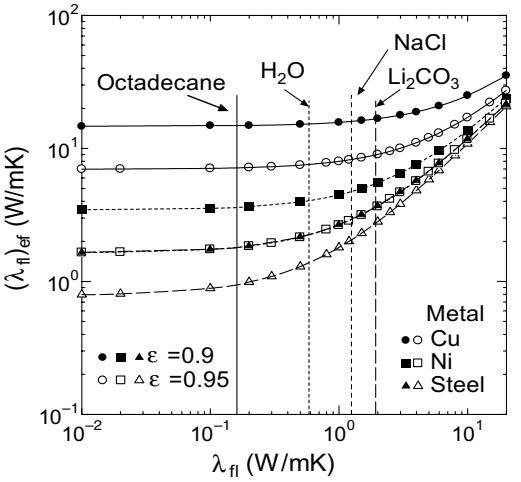


Fig. 2. Plot of effective thermal conductivity of composite PCM against $\lambda_{fl}$.

based on which the heat transfer coefficient was changed. Considering the melting temperatures of $Li_2CO_3$ and NaCl, water can not be used as HTF for commercially used PCMs. However, since the heat transfer coefficient of water is higher than those of air and helium at the same Reynolds number, the heat transfer coefficient of water was applied for the evaluation of the effect of the high heat transfer coefficient on melting of $Li_2CO_3$ and NaCl compared with other PCMs. In the present study, we call this analysis for the water case. In the analysis, temperatures were set as $T_\infty - T_f = 5$ °C and $T_i - T_f = -5$ °C. Thermal radiation was neglected in the analysis. For comparison with experimental results only, diameters $D_o$ of circular cylindrical capsules 8 mm, 10 mm and 1 mm in wall thickness were used, and thermal radiation was considered. Thermal emissivity of the apparatus surrounding the circular capsule was set at 0.85.

### 2.4. Comparison with experiment

In order to study the melting characteristics of the PCM, a melting experiment using forced convection was performed with water as the PCM filled in the circular capsule. The circular capsules were 8 mm and 10 mm in outer diameters and 1 mm in wall thickness. The capsule was set in the middle of a rectangular channel made of acrylic resin with cross section of 100 mm × 100 mm and 1000 mm in length [14]. In the experiment, the temperature of the central axis and surface temperatures at intervals of 90° from the stagnation point were measured. The shape of solid liquid boundary was visualized. The Reynolds number was made 300, 3000, and 7500.

## 3. Results and discussion

### 3.1. Comparison of experiment with analysis

Fig. 3 shows a plot of temperature against time for case of $D_o$ = 8 mm and $Re$ = 300. Marks show the experimental results. The two dotted lines in the figure show surface and center temperature obtained by the analysis with a uniform heat transfer coefficient and other lines show the analysis with a non-uniform heat transfer coefficient. Flow direction and positions where temperature was measured are indicated by the marks and lines as shown at the bottom of the figure. In the experiment, porous metal was not used. In this case, natural convection in the capsule was neglected in the estimate because the Rayleigh number, based on $D_i$, was very small in the capsule [14]. Analysis agreed well with the experimental results.

Fig. 4 compares the shape of liquid–solid boundary found in the experiment and in the analysis for the case where $D_o$ = 10 mm, $Re$ = 300 and time = 1200 s. Air flows from left to right in the figure. In the upper figure, a small air bubble can be seen near the inner wall. Numeric values in the bottom figure designate solid fraction. Good agreement between analysis and experiment can be seen.

### 3.2. Analytical results and discussion

#### 3.2.1. Effect of thermal conductivity on melting time

Hereafter, the Discussion is confined to the results based on the uniform heat transfer coefficient, unless stated otherwise.

Figs. 5 and 6 show the melting time plotted against effective thermal conductivity $(\lambda_{fl})_{ef}$ for composite PCMs

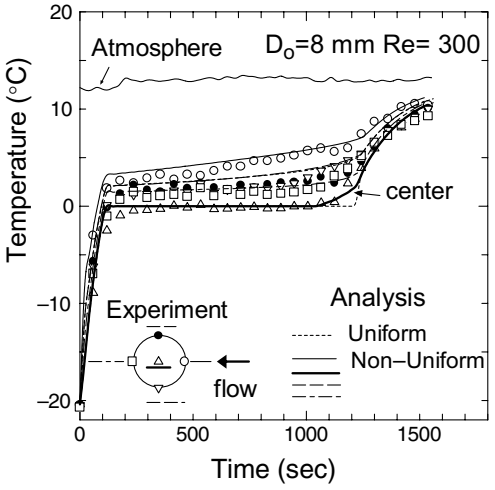


Fig. 3. Comparison of analysis with experiments ($D_o$ = 8 mm, $D_i$ = 6 mm, $Re$ = 300, PCM = water, HTF = air).

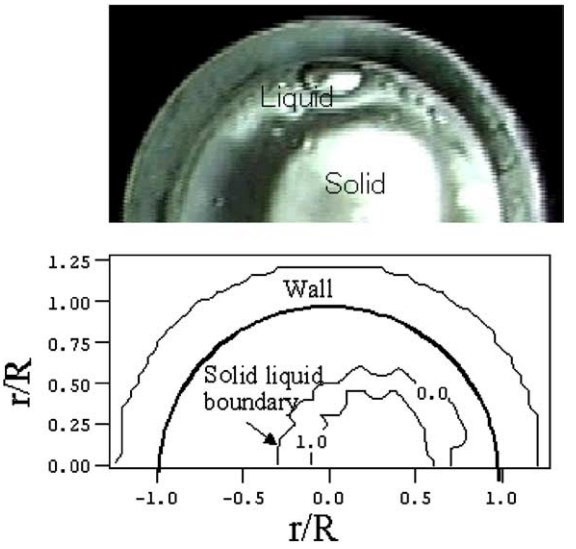


Fig. 4. Comparison of phase change boundary of experiment and of numerical analysis ($D_o$ = 10 mm, $D_i$ = 8 mm, $Re$ = 300, $t$ = 1200 s).

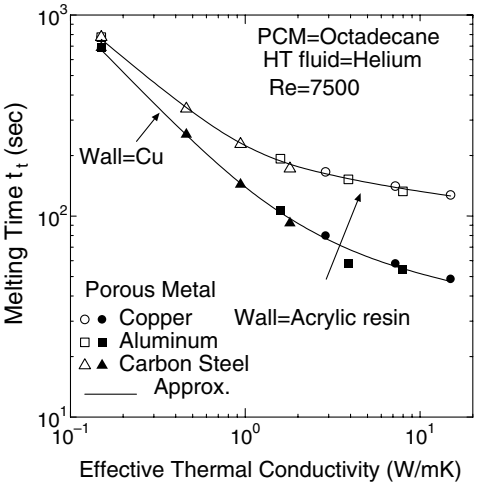


Fig. 5. Plot of melting time against $(\lambda_{fl})_{ef}$ (PCM = octadecane, HTF = helium, $Re$ = 7500).

of octadecane and $Li_2CO_3$, respectively, with helium as HTF and Reynolds number at $Re$ = 7500. Open and solid marks correspond to the walls of acrylic resin and copper, respectively. Four plot points of one mark-shape ranging from higher to lower value of abscissa correspond to $\varepsilon$ = 0.9, 0.95, 0.98 and 1.0, in order. The solid line shows the results of approximate analysis for copper based composite PCM. The results of the approximate analysis is about 4% smaller than that of the numerical analysis. As shown in the figure, melting time reduces with increase in effective thermal conductivity, but it

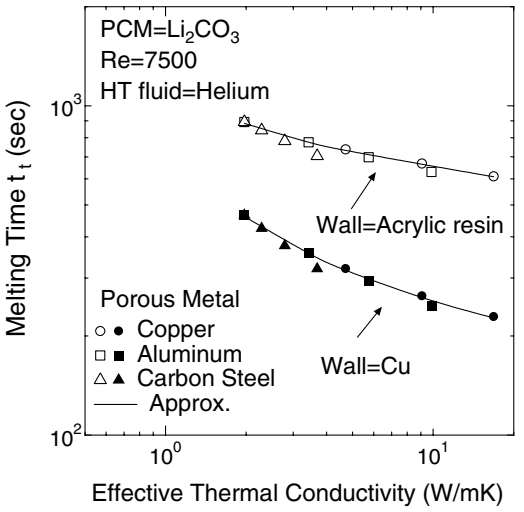


Fig. 6. Plot of melting time against $(\lambda_{fl})_{ef}$ (PCM = $Li_2CO_3$, HTF = helium, $Re$ = 7500).

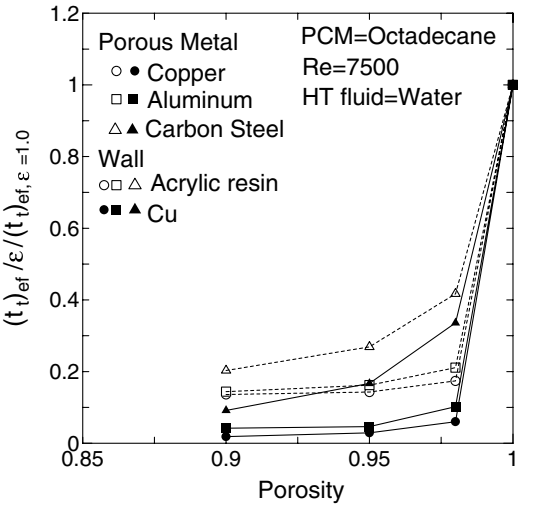


Fig. 7. Plot of $(t_t)_{ef}/\varepsilon/(t_t)_{ef,\varepsilon=1}$ against porosity (PCM = octadecane, HTF = water, $Re$ = 7500).

should be noticed that this reduction reflects the decrease in the amount of PCM with decrease in porosity to some extent. Reduction ratio of melting time decreases with increase in effective thermal conductivity. Melting time is longer in the case of the acrylic wall than the case of copper wall.

The value of $(t_t)_{ef}/\varepsilon$ can be regarded as close to the effective melting time of a PCM whose latent heat is the same as a pure PCM and whose other thermal properties are equal to effective values. The ratio of effective melting time $(t_t)_{ef}/\varepsilon/(t_t)_{ef,\varepsilon=1}$ which is the effective melting time normalized by $(t_t)_{ef,\varepsilon=1}$, melting time of $\varepsilon = 1$, is shown in Figs. 7 and 8 plotted against porosity for the composite PCM of octadecane and $Li_2CO_3$ and with water as HTF, at $Re$ = 7500. In case of octadecane, the ratio of effective melting time is as low as 0.1 even if porosity is near unity ($\varepsilon = 0.98$) as shown in Fig. 7. In the case of the $Li_2CO_3$, the ratio of effective melting time is not so low as the case of octadecane, but even here it decreases to 0.2 where $\varepsilon = 0.9$ (Fig. 8). The results show that the influence of the effective thermal conductivity on the melting time is higher for the PCM of low thermal conductivity than for that of high thermal conductivity. From Eq. (11), heat resistance of wall can be neglected when the wall thickness is decreased and metal with high thermal conductivity is adopted. Also, Eq. (11) shows that reduction in the ratio of melting time increases with increase in heat transfer coefficient. The ratio of effective melting time can be obtained by Eq. (11).

$$\frac{(t_t)_{ef}}{\varepsilon(t_t)_{ef,\varepsilon=1}} = \frac{\lambda_{fl}/(\lambda_{fl})_{ef} + 4/Bi_{fl} + (2\lambda_{fl}/\lambda_w)\ln(D_o/D_i)}{1 + 4/Bi_{fl} + (2\lambda_{fl}/\lambda_w)\ln(D_o/D_i)} \tag{19}$$

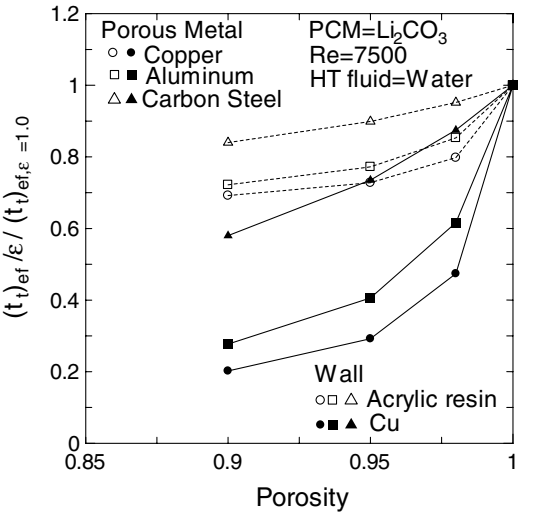


Fig. 8. Plot of $(t_t)_{ef}/\varepsilon/(t_t)_{ef,\varepsilon=1}$ against porosity (PCM = $Li_2CO_3$, HTF = water, $Re$ = 7500).

when $Bi_{fl}$ and $\lambda_w$ are large, the following equation is obtained:

$$\frac{(t_t)_{ef}}{\varepsilon(t)_{ef,\varepsilon=1}} \approx \frac{1}{(\lambda_{fl})_{ef}/\lambda_{fl}} \tag{20}$$

Figs. 9 and 10 show a plot of $t_{eff}/\varepsilon/(t_{eff})_{\varepsilon=1}$ against $(\lambda_{eff})_{ef}/\lambda_{fl}$ for copper wall and HTF of water and air at $Re$ = 7500, respectively. In the figure, the solid lines are those of Eq. (19) using copper saturated composite PCM and the dotted line is that of Eq. (20). Fig. 9 shows results where there is high heat transfer coefficient, i.e., high $Bi_{fl}$, and agrees comparatively well with Eq. (20).

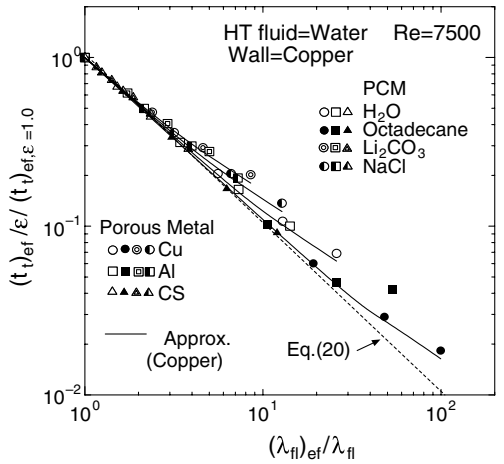


Fig. 9. Plot of $(t_t)_{ef}/\varepsilon/(t_t)_{ef,\varepsilon=1}$ against $(\lambda_{fl})_{ef}/\lambda_{fl}$ (HTF = water, $Re$ = 7500, wall = copper).

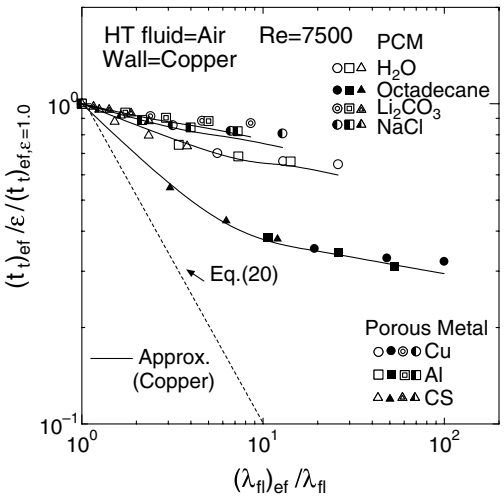


Fig. 10. Plot of $(t_t)_{ef}/\varepsilon/(t_t)_{ef,\varepsilon=1}$ against $(\lambda_{fl})_{ef}/\lambda_{fl}$ (HTF = air, $Re$ = 7500, wall = copper).

On the other hand, Fig. 10 shows results where there is lower heat transfer coefficient, i.e., low $Bi_{fl}$, and does not agree with Eq. (20) and reduction of the ratio of melting time is small compared with Fig. 9. For PCM with somewhat higher thermal conductivity than octadecane such as $Li_2CO_3$ and NaCl, the reduction of the ratio of effective melting time is small, at most 20%. Thus, in these conditions, high heat transfer coefficient is necessary for a higher rate of reduction of melting time.

### 3.2.2. Effect of non-uniform heat transfer coefficient

Table 3 shows results of numerical and approximate analysis of melting time for the case of the uniform heat transfer coefficient for a copper saturated composite PCM of water and octadecane with porosities of $\varepsilon = 0.9, 1.0$. In the table, the results were normalized with the results of numerical analysis based on the non-uniform heat transfer coefficient.

Table 3
Melting time based on the uniform heat transfer coefficient $h_0$ normalized according to values of the non-uniform heat transfer coefficient $h(\theta)$ (porous metal: copper; Num., App.: numerical and approximate analysis. Oct.: octadecane)

| HTF | PCM | Wall $\varepsilon$ | Acrylic resin | | Copper | |
|---|---|---|---|---|---|---|
| | | | Num. | App. | Num. | App. |
| Water | $H_2O$ | 0.9 | 0.967 | 0.956 | 0.996 | 0.965 |
| | $H_2O$ | 1 | 0.996 | 0.954 | 1.029 | 0.989 |
| | Oct. | 0.9 | 0.966 | 0.956 | 0.997 | 0.966 |
| | Oct. | 1 | 1.026 | 1.002 | 1.011 | 0.987 |
| He | $H_2O$ | 0.9 | 0.973 | 0.967 | 1.025 | 1.012 |
| | $H_2O$ | 1 | 0.922 | 0.891 | 1.03 | 0.99 |
| | Oct. | 0.9 | 0.966 | 0.959 | 1.024 | 1.008 |
| | Oct. | 1 | 0.954 | 0.928 | 1.014 | 0.982 |
| Air | $H_2O$ | 0.9 | 0.977 | 0.974 | 1.022 | 1.016 |
| | $H_2O$ | 1 | 0.963 | 0.946 | 1.021 | 0.998 |
| | Oct. | 0.9 | 1.006 | 1.002 | 1.021 | 1.01 |
| | Oct. | 1 | 0.918 | 0.894 | 1.017 | 0.983 |

Fig. 11 shows plots of angular dependence of heat flux on the acrylic wall against time for case of octadecane as PCM and water as heat transfer fluid at $Re$ = 300. The angle was measured from the stagnation point. In the figure, heat flux can be obtained by multiplying thermal conductivity $\lambda_g$ with ordinate value. Fig. 11(a) is the case of copper saturated composite PCM of octadecane with $\varepsilon = 0.9$ and (b) is the case where $\varepsilon = 1.0$. When thermal conductivity of the PCM and the wall is large enough, non-uniform heat flux on the wall surface transferred from the fluid is immediately transferred into the PCM, and surface temperature is kept uniform. Therefore, the conditions created by the uniform and non-uniform heat transfer coefficients ultimately converge. In practice, the results of the uniform and non-uniform heat transfer coefficients agree within about 2% for the case of copper saturated composite PCM and copper wall (see Table 3). Even in case of the acrylic wall, if the composite PCM has high effective thermal conductivity, non-uniform heat flux distribution on the wall was kept during melting (Fig. 11(a)). However, when thermal conductivity of PCM is low ($\varepsilon = 1.0$), initially non-uniform surface heat flux becomes nearly uniform with passage of time because at a surface where there is high heat transfer coefficient, local surface temperature at the early stage of melting is increased by high heat input, then heat input is decreased and reaches equilibrium due to decrease in temperature difference $T_\infty - T_w$ (Fig. 11(b)). In the analysis, melting time was longer for non-uniform heat transfer coefficient. How-

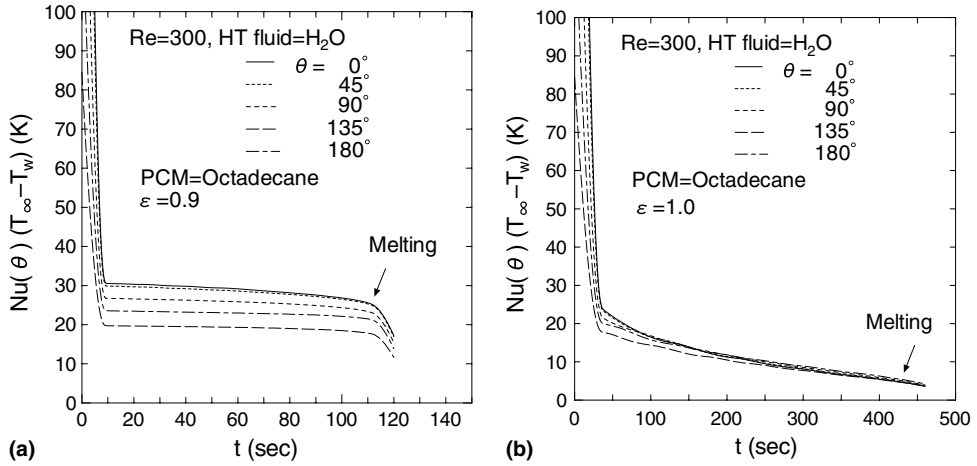


Fig. 11. Plot of angular distribution of heat flux on the circular capsule (HTF = water, $Re$ = 300, PCM = octadecane, metal = porous copper): (a) for case of $\varepsilon = 0.9$; (b) for case of $\varepsilon = 1.0$.

ever, the difference between uniform and non-uniform was 8% at the maximum. Therefore, it can be concluded that the difference in melting time between the two cases is at most 10%. The degree of variation in the non-uniform heat transfer coefficient used in the present study likely is the highest such degree among many types of arrangements. Therefore, a uniform heat transfer coefficient can be used for the design analysis of capsule type heat storage system.

### 3.2.3. Time variation of surface heat flux

Melting time was considerably reduced when thermal conductivity was improved by the use of composite PCM. This is due to the increase in heat input to the capsule from HTF. The value of $q_{ef}/q$ was calculated, where $q_{ef}$ and $q$ are the surface heat fluxes for composite PCM and pure PCM, respectively. Fig. 12 shows a plot of $q_{ef}/q$ against time for copper saturated composite PCM of octadecane and $Li_2CO_3$ with porosity as a parameter and with helium as the HTF of $Re$ = 7500. As shown in the figure, $q_{ef}/q$ of composite PCM of octadecane exceeds ten even where $\varepsilon = 0.98$. Even for the case of $Li_2CO_3$, $q_{ef}$ increases about two times in average at $\varepsilon = 0.95$. Sasaguchi et al. [1] measured heat flux on a finned surface of a heat storage circular cylinder saturated with eicosane whose thermal properties are almost same as octadecane and where porosity of the fin was 0.964. They reported that the heat flux increased about 2.4 times. This result indicates that a composite PCM is more effective for reducing melting time than a finned surface. The main reasons seem to be as follows: the effect of a finned surface is mainly to expand heat transfer surface, however, surface temperature is increased by the heat input from the wall when thermal conductivity is low, which causes reduction of heat input as time passes. However, when the effective thermal conductivity is high, heat flowing in from the surface is immediately transferred into the PCM and increase in surface temperature is suppressed, so that high heat input can be maintained for a long period. Therefore, improvement of thermal conductivity is very effective for reducing melting time.

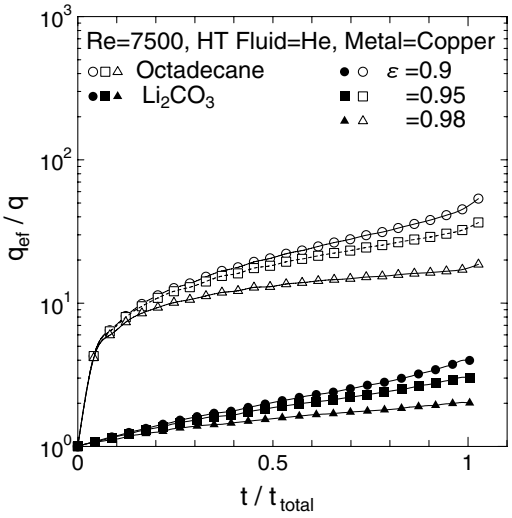


Fig. 12. Ratio of heat flux of composite heat storage unit with porous metal to that without porous metal (PCM: octadecane, $Li_2CO_3$; HTF: helium; $Re$ = 7500).

### 3.3. Estimation of optimal porosity

### 3.3.1. Effective condition of composite PCM

We now will look for the conditions where improvement of thermal conductivity yields considerable

reduction of melting time. In the present study, melting time determined by Eq. (11) using approximate analysis showed good agreement with numerical results for small Stephan number. Eq. (11) can be rewritten as

$$t_t = \frac{D_i^2(\rho)_{ef}}{16}\left\{\frac{(L)_{ef}}{(T_\infty - T_f)}\left(\frac{1}{(\lambda_{fl})_{ef}} + \frac{4}{\lambda_g Nu_d} + \frac{2}{\lambda_w}\ln\frac{D_o}{D_i}\right) - c\left(\frac{1}{(\lambda_{fs})_{ef}} + \frac{D_o}{D_i}\frac{4}{\lambda_g Nu_d} + \frac{D_o}{D_i}\frac{2}{\lambda_w}\ln\frac{D_o}{D_i}\right)\cdot\ln\theta_f\right\} \quad (21)$$

The second term of the right-hand side of Eq. (21) designates sensible heat and is negligible compared with the first term. Considering necessary conditions for heat storage of large $\rho$, $c$, and $L$ and also considering that $2/\lambda_w \ln D_o/D_i$ in the first term of the right-hand side can be zero for large $\lambda_w$ and where $D_o/D_i \to 1$, the condition for reducing melting time for selected PCM is that the value of the following equation is reduced:

$$1/(\lambda_{fl})_{ef} + 4/\lambda_g Nu_d$$

From the above equation, increase in effective thermal conductivity is more effective in reducing melting time when the first term of the above equation is larger than the second term, i.e., $1/(\lambda_{fl})_{ef} > 4/\lambda_g Nu_d$, which yields

$$Nu_d \geqslant 4\frac{(\lambda_{fl})_{ef}}{\lambda_g} \quad (22)$$

This indicates that a high heat transfer coefficient is effective even if thermal conductivity of PCM is low.

*3.3.2. Calculation of optimal porosity*

Essential conditions of a latent heat storage system are high heat storage capacity and high phase change rate. In order to keep high heat storage capacity, porosity should be near unity, whereas high phase change rate can be obtained by lower porosity due to decrease in the amount of PCM. Therefore an optimum porosity would have a mid range value. Estimation of it depends upon the design goal of the heat storage system: which is regarded to be more important, phase change velocity or heat storage capacity. In the present study, we propose a trial estimation on the basis of both conditions being equally important. Increasing heat capacity $Q$ and reducing effective melting time $(t_t)_{ef}/\varepsilon$ can be satisfied by decreasing $(t_t)_{ef}/\varepsilon Q$. Therefore, the optimal value of $\varepsilon$ can be obtained by minimizing $(t_t)_{ef}/\varepsilon Q$. When second term of Eq. (21) is neglected, minimizing $(t_t)_{ef}/\varepsilon Q$ is equivalent to minimizing the following term:

$$\left(\frac{1}{(\lambda_{fl})_{ef}} + \frac{4}{\lambda_g Nu_d} + \frac{2}{\lambda_w}\ln\frac{D_o}{D_i}\right)\frac{1}{\varepsilon} \quad (23)$$

Here, we set $a = \frac{4}{\lambda_g Nu_d} + \frac{2}{\lambda_w}\ln\frac{D_o}{D_i}$, $X = (\lambda_{fl})_{ef}$, and then Eq. (23) can be written as $(1/X + a)/\varepsilon$. Minimizing this is the same as maximizing the following equation:

Table 4
One example of the optimum porosity (Ac = acrylic resin)

| PCM | Metal | Wall | HTF | $Re$ | $(\varepsilon)_{optimum}$ |
|---|---|---|---|---|---|
| $H_2O$ | Cu | Ac | Air | 300 | 0.981 |
| | | Cu | Air | 300 | 0.981 |
| | | Ac | Water | 7500 | 0.921 |
| | | Cu | Water | 7500 | 0.739 |
| Octadecane | Cu | Ac | Air | 300 | 0.995 |
| | | Cu | Air | 300 | 0.994 |
| | | Ac | Water | 7500 | 0.933 |
| | | Cu | Water | 7500 | 0.748 |

$$f(\varepsilon) = \frac{\varepsilon X}{1 + aX}$$

Therefore this problem reduces to obtain $\varepsilon$ which satisfies following equation:

$$X(1 + aX) + \varepsilon\frac{dx}{d\varepsilon}\frac{dX}{dx} = 0$$

where $x$ is the same as in Eq. (18). Results are shown in Table 4. The optimum $\varepsilon$ becomes high for a low heat transfer coefficient and low for a high heat transfer coefficient.This is because melting time is mainly reduced by decrease in the amount of PCM rather than the increase in effective thermal conductivity when heat transfer coefficient is low, and, the opposite is the case for high heat transfer coefficient. Therefore, optimal value is dependent on the manner of application of the system.

## 4. Conclusions

Efficiency of effective thermal conductivity of PCM on phase change characteristics was studied by analyzing the melting characteristics of circular cylindrical heat storage capsules filled with a composite PCM consisting of highly porous metal in which is saturated PCM. In the analysis, octadecane, water, $Li_2CO_3$ and NaCl were selected as PCMs, copper, aluminum and carbon steel as porous metals, and air, helium and water as HTF. The following conclusions were obtained:

(1) Melting time can be considerably reduced by increasing the effective thermal conductivity of composite PCM. The rate of reduction of melting time is noticeable as thermal conductivity of PCM is low and heat transfer coefficient on the surface is high.
(2) Melting time represented by the approximate analysis, Eq. (11), agrees well with numerical analysis for small Stephan number.
(3) Surface heat flux transferred by HTF to the capsules is about several to ten times higher with the use of composite PCM than using a finned surface. This shows that composite PCM is very effective to reduce phase change time.

(4) Melting time for the case of non-uniform heat transfer coefficient on the surface is at most 10% larger than the case of uniform heat transfer coefficient. Therefore, it suffices to use a uniform heat transfer coefficient for design of capsule type heat storage system.
(5) A trial estimation of optimal porosity was presented. The result shows that optimal porosity is near 1 for the case of low heat transfer coefficient. It decreases with increase in heat transfer coefficient.

## References

[1] K. Sasaguchi, H. Imura, H. Furusho, Heat transfer characteristics of fin tube type latent heat storage equipment, Trans. JSME B 52 (1986) 159–166 (in Japanese).
[2] A.G. Bathelt, R. Viacanta, Heat transfer and interface motion during melting and solidification around a finned heat source/sink, Trans. ASME C 103 (1981) 720–726.
[3] T. Hirata, H. Ueda, M. Fujiwara, Heat transfer of latent thermal energy storage capsules arranged in alignment with fluid flow, Trans. JSME B 53 (1987) 204–215 (in Japanese).
[4] S. Itoh, Heat transfer problems of a cylindrical capsule for latent heat thermal energy storage, Trans. JSME B 50 (1984) 556–561 (in Japanese).
[5] Y. Takahashi et al., Thermoanalytical investigation of fluoride composites for latent thermal storage, Thermochim. Acta 183 (1991) 299–311.
[6] Y. Hirasawa, T. Hamada, E. Takegoshi, An experimental study on melting process of ice containing conductive solids, Trans. JSME B 60 (1994) 2491–2496 (in Japanese).
[7] J. Fukai et al., Effect of carbon fibers on thermal response with heat storage material, Trans. Chem. Eng. 23 (1997) 82–87 (in Japanese).
[8] Y. Katto, H. Nishimura, Heat conduction with phase change, Trans. JSME 26 (1972) 715–719 (in Japanese).
[9] K. Kawashita, Heat conduction, p. 161, Ohm-sha (1966).
[10] A. Zukauskas, Heat transfer from tubes in crossflow, Adv. Heat Transfer 8 (1972) 133–138.
[11] E.R.G. Eckert, G. Soengen, Distribution of heat transfer coefficients around circular cylinders in crossflow at Reynolds numbers from 20 to 500, Trans. ASME 74 (1952) 343–347.
[12] E. Schmidt, K. Wenner, Forsch. Geb. Ingenierwes 12 (1941) 65–73.
[13] E. Takegoshi et al., A study on effective thermal conductivity of porous metals, Trans. JSME B 58 (1992) 879–884 (in Japanese).
[14] K. Iwasa, Y. Shiina, T. Inagaki, Melting of phase change fluid in heat storage capsules by convection, J. Flow Visual. Jpn. 19 (1999) 41–45 (in Japanese).